Korean J. Chem. Eng., **30**(5), 1162-1170 (2013)
DOI: 10.1007/s11814-013-0015-x

Pyrolytic characteristics of Jatropha seedshell cake in thermobalance and fluidized bed reactors

Sung Won Kim*, Dong Kyoo Park, and Sang Done Kim**†**

*Catalyst & Process R&D Center, SK Innovation, 140-1, Wonchon-dong, Yuseong-gu, Daejeon 305-712, Korea
**Department of Chemical and Biomolecular Engineering, Energy and Environmental Research Center, Korea Advanced Institute of Science and Technology (KAIST), 373-1, Guseong-dong, Yuseong-gu, Daejeon 305-701, Korea
(*Received 9 January 2013 • accepted 3 February 2013*)

Abstract−Pyrolytic kinetic parameters of Jatropha seedshell cake (JSC) were determined based on reaction mechanism approach under isothermal condition in a thermobalance reactor. Avrami-Erofeev reaction model represents the pyrolysis conversion of JSC waste well with activation energy of 36.4 kJ mol^{-1} and frequency factor of 9.18 s^{-1}. The effects of reaction temperature, gas flow rate and feedstock particle size on the products distribution have been determined in a bubbling fluidized bed reactor. Pyrolytic bio-oil yield increases up to 42 wt% at 500 °C with the mean particle size of 1.7 mm and gas flow rate higher than $3U_{mf}$, where the maximum heating value of bio-oil was obtained. The pyrolytic bio-oil is characterized by more oxygen, lower HHVs, less sulfur and more nitrogen than petroleum fuel oils. The pyrolytic oil showed plateaus around 360 °C in distribution of components' boiling point due to high yields of fatty acid and glycerides.

Key words: Pyrolysis, Jatropha, Bio-oil, Thermobalance, Fluidized Bed

INTRODUCTION

Biomass is one of the most important renewable alternative energy resources nowadays. A number of biomass resources such as agricultural waste, forestry waste and municipal and industrial wastes can be used for fuel production. Bio-fuels are clean energy sources since biomass is considered as CO_2 neutral with their low nitrogen and sulfur content compared with fossil fuels [1]. Jatropha oil is produced in mills by streaming and pressing the fruit. Significant amount of solid wastes, including shells, fiber and kernels, are generated, some of which is currently used as low energy efficiency fuel for boilers. Efficient management of the wastes like conversion to valuable product is required to improve process efficiency and economics in overall oil production [2]. Biomass conversion processes are mainly divided into two groups as biochemical (fermentation and anaerobic digestion) and thermochemical (combustion, gasification and pyrolysis) processes. Pyrolysis is one of the most promising technologies of biomass utilization, which is a thermal degradation of materials in the absence of oxygen. The pyrolysis converts the biomass to bio-oil, char and gases depending on the pyrolysis conditions. To maximize fuel gas yield, biomass is pyrolyzed at high temperature, low heating rate and longer vapor residence time, or to enhance char production at lower temperature and heating rate. To obtain high yields of bio-oil, the following conditions are required: moderate temperature, very high heating rates, short vapor residence time and rapid quenching of vapors. Bio-oil from pyrolysis is considered as a promising fuel because it can be easily transported, burnt directly in thermal power stations, injected into conventional petroleum refineries or upgraded to obtain light hydrocarbon fuels [3-5]. In addition, considerable research has recently focused on the distribution of various gas products, aiming to improve the yield of H_2 as clean energy source for H_2-powered engine and fuel cell [6-8]. The effects of pyrolysis parameters on oil yields from Jatropha waste in fixed and fluidized bed reactors have been widely studied [2,8]. However, these studies focus on obtaining an optimal operating condition for relatively high liquid yield. A comprehensive study including kinetic analysis and pyrolytic characteristics is required for practical development of Jatropha waste pyrolyzer with flexibility in operation, because its design and operation should be adjusted depending on the type of energy demand like liquid or gas fuels.

In this study, pyrolytic kinetic parameters of Jatropha seed shell cake were determined based on reaction mechanism approach in a thermobalance reactor. Also, the effects of various reaction conditions such as reaction temperature, mean particle size and gas flow rate on composition and yield of products were determined in a bubbling fluidized bed reactor.

EXPERIMENTAL

1. Pyrolysis Kinetics

The conversion (α) of a carbonaceous solid is defined as

$$\alpha = \frac{W_0 - W}{W_0 - W_\infty} \tag{1}$$

where W_0, W and W_∞ are the initial, instantaneous and final mass of sample, respectively.

The rate is expressed by the following Arrhenius equation:

$$\frac{d\alpha}{dt} = k(T)f(\alpha) = A\exp\left(\frac{-E}{RT}\right)f(\alpha) \tag{2}$$

Kinetics of carbonaceous pyrolysis is characterized by activation

†To whom correspondence should be addressed.
E-mail: kimsd45@kaist.ac.kr

Table 1. Commonly used conversion function for carbonaceous thermal decomposition reactions

Mechanism		f(α)	g(α)
Chemical reaction			
1	First order	$1-\alpha$	$-\ln(1-\alpha)$
2	Second order	$(1-\alpha)^2$	$(1-\alpha)^{-1}-1$
3	Third order	$(1-\alpha)^3$	$((1-\alpha)^{-2}-1)/2$
4	nth order	$(1-\alpha)^n$	$((1-\alpha)^{1-n}-1)/(n-1)$
Random nucleation and nuclei growth			
5	Avrami-Erofeev equation (n=2)	$2(1-\alpha)[-\ln(1-\alpha)]^{1/2}$	$[-\ln(1-\alpha)]^{1/2}$
6	Avrami-Erofeev equation (n=3)	$3(1-\alpha)[-\ln(1-\alpha)]^{2/3}$	$[-\ln(1-\alpha)]^{1/3}$
7	Avrami-Erofeev equation (n=4)	$4(1-\alpha)[-\ln(1-\alpha)]^{3/4}$	$[-\ln(1-\alpha)]^{1/4}$
Limiting surface reaction between both phases			
8	Contracting area	$2(1-\alpha)^{1/2}$	$1-(1-\alpha)^{1/2}$
9	Contracting volume	$3(1-\alpha)^{2/3}$	$1-(1-\alpha)^{1/3}$
Diffusion mechanism			
10	One-dimensional	$\alpha/2$	α^2
11	Two-dimensional	$[-\ln(1-\alpha)]^{-1}$	$\alpha+(1-\alpha)[\ln(1-\alpha)]$
12	Three-dimensional	$3/2(1-\alpha)^{2/3}/(1-(1-\alpha)^{1/3})$	$(1-(1-\alpha)^{1/3})^2$
13	Ginstling-Brounshtein equation	$3/2(1-\alpha)^{1/3}/(1-(1-\alpha)^{1/3})$	$1-2/3\alpha-(1-\alpha)^{2/3}$

energy (E), frequency factor (A) and reaction model function (f, conversion function) so-called as kinetic triplet. Re-arranging and integrating Eq. (2), the following equation can be obtained:

With initial condition, t=0, α=0,

$$g(\alpha)=\int_0^{\alpha}\frac{1}{f(\alpha)}d\alpha=A\exp\left(\frac{-E}{RT}\right)t \tag{3}$$

The reaction model can be expressed in various forms depending on the rate limiting step; the models generally used are listed in Table 1 [9,10]. From the isothermal experiments, the reduced time plots (RTPs) were constructed by plotting α as a function of reduced time (t/t_α), where t_α is the time that it takes to attain a specific conversion of 0.9 in Fig. 1. Reaction model can be chosen among the various reaction models by means of comparing experimental RTPs with the theoretical ones in Table 1. Goodness of fit of the theoretical RTP to the experimental one can be judged by the residual sum of squares as

$$S^2=\frac{1}{N-1}\sum_{j=1}^{N}\left(\frac{t_j}{t_{0.9}}-\frac{g(\alpha_j)}{g(0.9)}\right)^2 \tag{4}$$

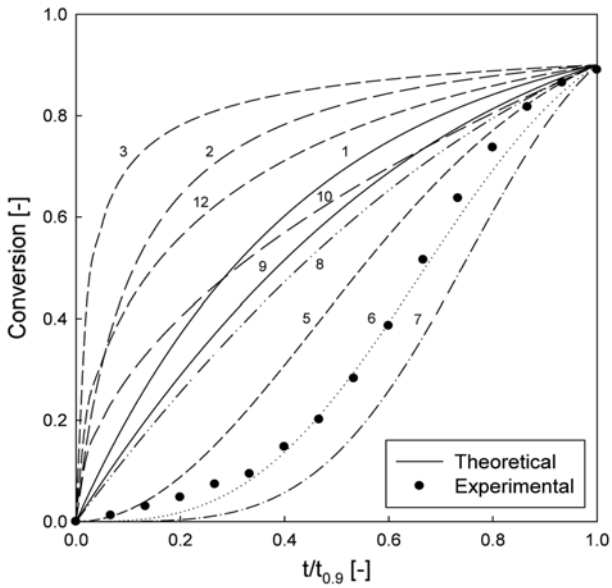

Fig. 1. Experimental and theoretical reduced time plots (RTPs) for the reaction model in Table 1.

2. Raw Materials

Jatropha seed shell waste, which is acquired as a byproduct of oil extraction, was chosen as carbonaceous resource. The sample was acquired from an oil extraction plant in Indonesia. Proximate and ultimate analyses and chemical compositions are shown in Table 2. Proximate analysis was performed by an analyzer of model Ther-

Table 2. Proximate and ultimate analyses of Jatropha seed shell waste

Proximate analysis (wt%)		Ultimate analysis (wt%)		Component analysis (wt%)	
Volatile matter	68.23	C	49.52	Cellulose	36.64
Fixed carbon	18.12	H	6.82	Hemicellulose	4.82
Ash	5.40	O	40.34	Lignin	39.61
Moisture	8.24	N	3.19	Others	18.94
HHV (cal/g)	4783.8	S	0.14		

mostep (ELTRA) according to the ASTM 5142 standard test method. The proximate analysis showed volatiles (mainly organic), of 68.23 wt% in Jatropha seed shell. Elemental composition by ultimate analysis was obtained by an elemental analyzer of model EA 1108 (Fisons Instruments) according to the ASTM D3176 standard procedures. The elemental analysis showed that Jatropha waste mainly consisted of carbon and oxygen. Chemical composition for macrocomponents of the sample was identified using Tappi T203 and T222 standard methods. Chemical composition analysis showed the waste to have high cellulose and lignin. The waste features high content of other organic compounds which do not have constructive properties in biomass. The compound seems to be oil or fatty molecule because Jatropha seed shell waste is remnant from oil extraction and likely contains oil residue in the shell cakes. To eliminate the effect of moisture content prior to each test, sufficient amounts of fuel samples were dried at 105 °C for several hours and then stored in desiccators to prevent extra absorption of moisture from the atmosphere. Jatropha waste particle was screened using standard sieves to obtain mean particle sizes of 0.8, 1.2, 1.5, 1.7, 2.0, 2.6, 3.4, 6.0 mm. To compare the properties of the pyrolytic oil with petroleum fuel oils, high sulfur diesel (HS diesel) and heavy fuel oil (HFO) samples with low and high sulfur content were acquired from SK innovation's Ulsan complex, Korea.

3. Experimental Apparatus

3-1. Thermobalance Reactor

To obtain the kinetics of pyrolysis, Jatropha waste was pyrolyzed in a thermobalance reactor at isothermal conditions of 400-700 °C as shown in Fig. 2(a). The reactor was heated to a desired temperature under N_2 flow to eliminate the O_2 for more than 10 min. Samples were placed in a stainless steel wire mesh basket suspended from an electric balance. During the reaction, weight variation of the sample was continuously recorded by a personal computer. Details of the thermobalance and the experimental procedure can be found elsewhere [11].

3-2. The Fluidized Bed Reactor

Pyrolysis of Jatropha was carried out in a bubbling fluidized bed reactor as shown in Fig. 2(b). The fluidized bed reactor consisted of the main fluidized bed, biomass feeder and products recovery section. The main fluidized bed (0.1 m-I.D.×0.15 m-high) and the upper part of the bed were expanded (0.2 m-I.D.×0.6 m-high) for reduction of particle entrainment from the bed. A bubble cap type gas distributor having seven caps was placed between the main column and a gas plenum for uniform gas distribution in the bed. Silica sand was used as a bed material, whose mean particle diameter was 278 mm (U_{mf}=0.055 m/s). Pyrolysis tests were conducted at 400-700 °C with N_2 flow rates of 38-116 L/min at 25 °C (superficial gas velocities of 0.083-0.248 m/s), corresponding to ca. 1.5-4.5 U_{mf} at 500 °C and bubbling fluidization regime. Mean biomass size of 6.0 mm was chosen for study in reference condition, considering practical treatment of feedstock for industrial application. Static bed heights of 0.3 m were maintained in each test, giving residence times of the pyrolysis vapor out of the bed of *ca.* 5.2-15.4 s considering expansion of the fluidized bed, which depended on temperature and gas velocity. An electric heater was installed at the reactor wall to heat the bed to the desired temperature. At the desired temperature, the sample was fed into the bed by a screw feeder installed at the top of the fluidized bed reactor. Entrained particles and unreacted char

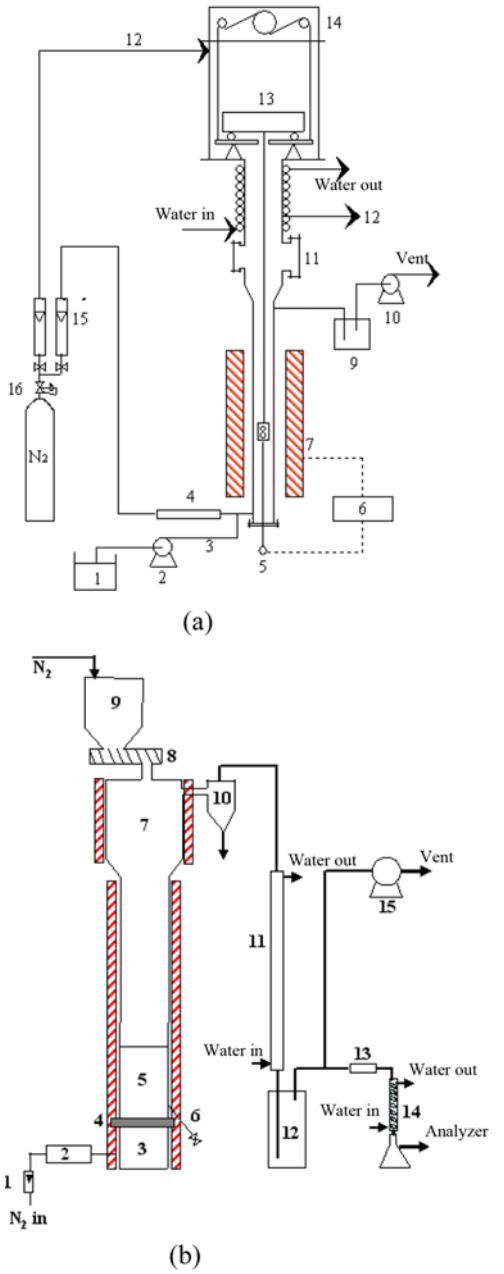

Fig. 2. Schematic diagram of experimental apparatuses.

(a) Thermobalance reactor

1. Water reservoir
2. Masterflex pump
3. Steam generator
4. Preheater
5. Thermocouple
6. Temperature controller
7. Electric heater
8. Sample basket
9. Cold trap
10. Vacuum pump
11. Hatch
12. N_2 purge line
13. Electric balance
14. Winch assembly
15. Flow meter
16. Regulator

(b) Fluidized bed reactor

1. Flowmeter
2. Preheater
3. Air box
4. Distributor
5. Main bed
6. Bed drain
7. Freeboard
8. Screw feeder
9. Hopper
10. Cyclone
11. Heat exchanger
12. Collector
13. Dust filter
14. Condenser
15. I.D. fan

were collected by a cyclone. To prevent condensation of oil products, the cyclone was insulated and maintained over 300 °C. Flue gases and vapors were cooled through a heat exchanger and condenser, and then the oil products were collected. The collected bio-oil was characterized by the standard procedures used to assess conventional petroleum fuel. The following properties were determined: (a) specific gravity (ASTM D-4052), (b) calorific values (ASTM D-2222), (c) total acid number or TAN (ASTM D-664), (d) distillation curve (ASTM D-2887) and (e) elemental analysis by elemental analyzer (EA1110, CE instruments). Non-condensable gases were sampled at the outlet of the condenser. Two types of gas analyzers were used to determine composition of the product gas. Concentrations of CO_2, CO and CH_4 were analyzed by infrared gas analyzer (Fuji electric system Co.), and H_2 concentration was determined by thermal conductivity gas analyzer (Fuji electric system Co.). The oil phase was characterized by GC/MS analysis (GC/MS 5972, Agilent) to determine its qualitative and quantitative composition.

RESULTS AND DISCUSSION

1. Pyrolysis Kinetics

Kinetics of Jatropha pyrolysis was determined in thermobalance at isothermal conditions, where mass and heat transfer limitation can be neglected since size and weight of the sample are small.

To define the chemical reaction control regime, the effects of the initial sample weight and mean particle size on the reactivity were determined at 500 °C (Fig. 3).

Reactivity of pyrolysis can be defined as [11],

$$R = -\frac{1}{W_0}\left(\frac{dW}{dt}\right) \quad (5)$$

where, R is reactivity of pyrolysis, W_0 is initial weight of sample on a dry and ash free basis, and dW/dt is average rate of weight loss up to the maximum rate of reaction.

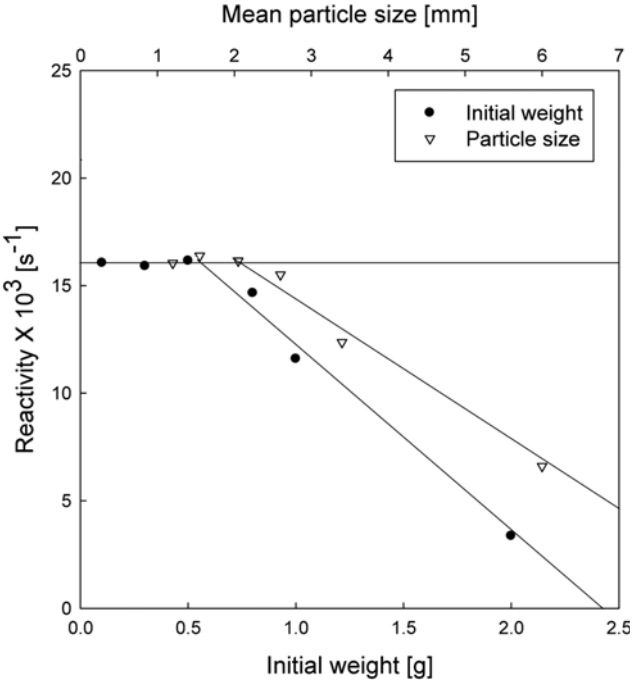

Fig. 3. Reactivity of Jatropha seed shell waste at different particle size and initial weight.

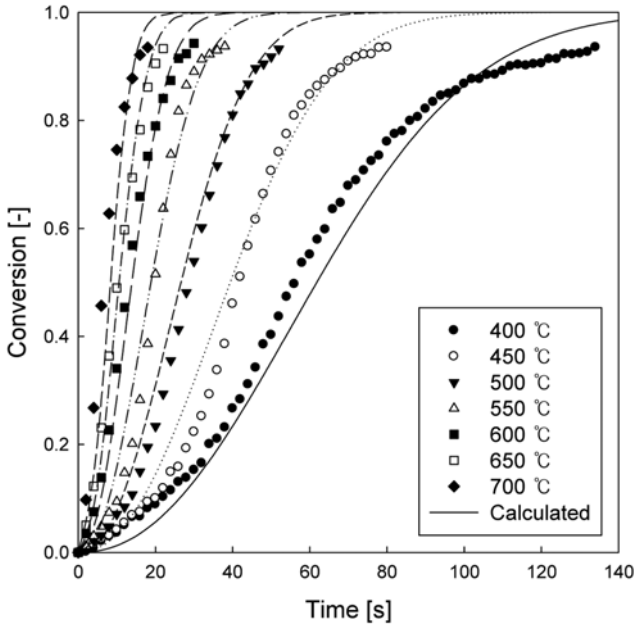

Fig. 4. Comparison of the experimental and calculated conversion by the Avrami-Erofeev model.

It can be seen that the reactivity decreases with increasing the initial sample weight more than 0.5 g and the mean particle size larger than 2.0 mm. Therefore, pyrolytic kinetics of Jatropha should be determined at the initial sample weight of 0.5 g and the mean particle size of 1.2 mm. N_2 flow rate was fixed to 5.5 cm/s where the effect of gas flow rate on residence time and the secondary reactions is negligible.

Conversions of Jatropha pyrolysis at isothermal temperatures of 400-700 °C are shown in Fig. 4. To predict the conversion of Jatropha pyrolysis, proper conversion function can be determined by comparison between the experimental and theoretical reduced time plots (RTPs) (Fig. 1). The experimental data is in good agreement with those from the Avrami-Erofeev model, whose reaction mechanism is random nucleation and nuclei growth. Main components of biomass such as cellulose and lignin are melted by heat prior to volatilization. Volatiles formed in melting are accumulated until a critical concentration is reached. At the critical concentration of volatiles, bubbles may begin to nucleate and grow until being released through the melt surface [10]. Thus, bubble nucleation is responsible for a major pyrolysis mechanism of Jatropha. By utilizing the Avrami-Erofeev model with an averaged exponent of 2.2, activation energy and frequency factor are determined to be 36.4 kJ/mol and 9.18 s^{-1}, respectively.

The pyrolysis rate of Jatropha can be represented by the following kinetic equation:

$$\frac{d\alpha}{dt} = 9.18 \times \exp\left(\frac{-36.4 \times 10^3}{RT}\right) \times 2.2(1-\alpha)(-\ln(1-\alpha))^{0.54} \quad (6)$$

The activation energy can be determined by the model-free isoconversional method, which assumes that reaction temperature and heating rate have no effects on the reaction mechanism [9].

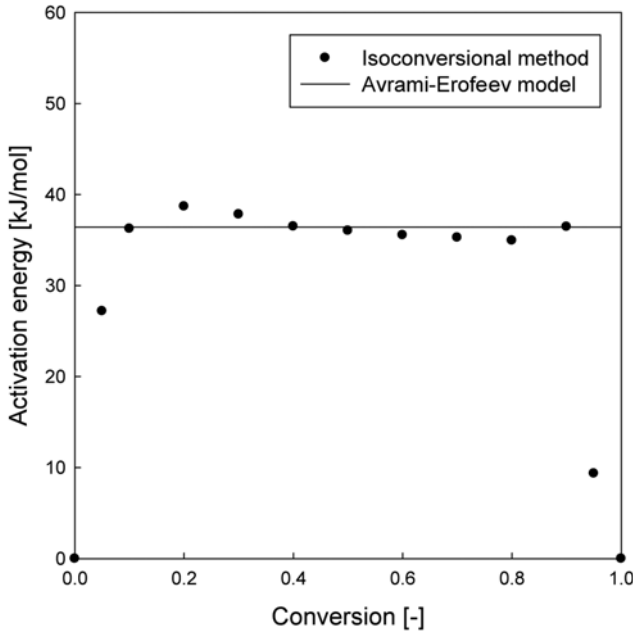

Fig. 5. Comparison of activation energies calculated by the Avrami-Erofeev model and model-free method.

$$\ln t_{\alpha,i} = -\ln\left(\frac{A_\alpha}{g(\alpha)}\right) + \left(\frac{E_\alpha}{R}\right)\frac{1}{T_i} \quad (7)$$

where, $t_{\alpha,i}$ is reaction time to a given conversion of a at temperature T_i, and A_α and E_α are frequency factor and activation energy at a given conversion a.

The averaged activation energy calculated by the model-free method is 36.38, which is very similar to that calculated by the Avrami-Erofeev model (Fig. 5). In addition, the predicted conversion is in good agreement with the experimental data (Fig. 4).

2. Pyrolysis in a Fluidized Bed Reactor

2-1. Effect of Temperature

The effect of temperature on the product yields of Jatropha pyrolysis is shown in Fig. 6(a) at a fluidizing gas velocity of 16.5 cm/s ($3U_{mf}$) and a mean particle size of 6.0 mm. As can be seen, char yield decreases down to 0.30 g/g_{sample} continuously with increasing temperature. As the temperature is increased, the primary thermal decomposition and the subsequent reactions of char with volatiles increase to produce more volatiles [12]. Bio-oil yield has a maximum value of 0.38 g/g_{sample} at 500 °C. At lower temperature, the oil production is less due to the incomplete pyrolysis. With increasing temperature above 500 °C, heavy molecular weight hydrocarbons are decomposed by the secondary thermal decomposition and the cracking reactions to convert it into gas products [13,14]. It causes decreasing the oil yield down to 0.29 g/g_{sample}; however, conversion to gaseous products increases over 500 °C, and thus gas yield rapidly increases to 0.41 g/g_{sample} at 700 °C. The effect of temperature on yields of gas components is shown in Fig. 6(b). At lower temperature, CO_2 is the major product that is about 80 wt% of total gas yield. As the temperature is increased, CO_2 yield increases about 30%, whereas its proportion decreases in the total gas yield down to 58 wt%. On the other hand, CO and CH_4 yields increase more than three and six times, and they are approximately 40 wt% of the total gas yield at 700 °C. At lower temperature, cross-linking reactions and primary decomposition of hemicellulose and cellulose in lignocellulosic biomass produce a large amount of oxygen containing gases due to their abundant oxygenated functional groups. As the pyrolysis temperature is increased, however, the secondary reactions of volatiles are dominant followed by reduction of CO_2; therefore, CO and CH_4 become the main components of the product gases [15,16]. Hydrogen is produced by extensive depolymerization of the phenyl groups which constitute mostly in lignin of biomass, and the severe secondary reactions of heavy molecular weight hydrocarbons in the evolving volatiles at high temperature produce additional H_2 [17]. Therefore, H_2 yield increases more than 20 times and it contributes 2.65 wt% of total gas yield at 700 °C.

In Fig. 7, bio-oil yields in this study are compared with those of other biomass pyrolysis in fluidized bed reactors [13,14,18] and fixed bed reactors [8,19]. The conditions of pyrolysis and the chemical compositions used in these previous studies are summarized in Table 3. Biomass pyrolysis is influenced by many parameters includ-

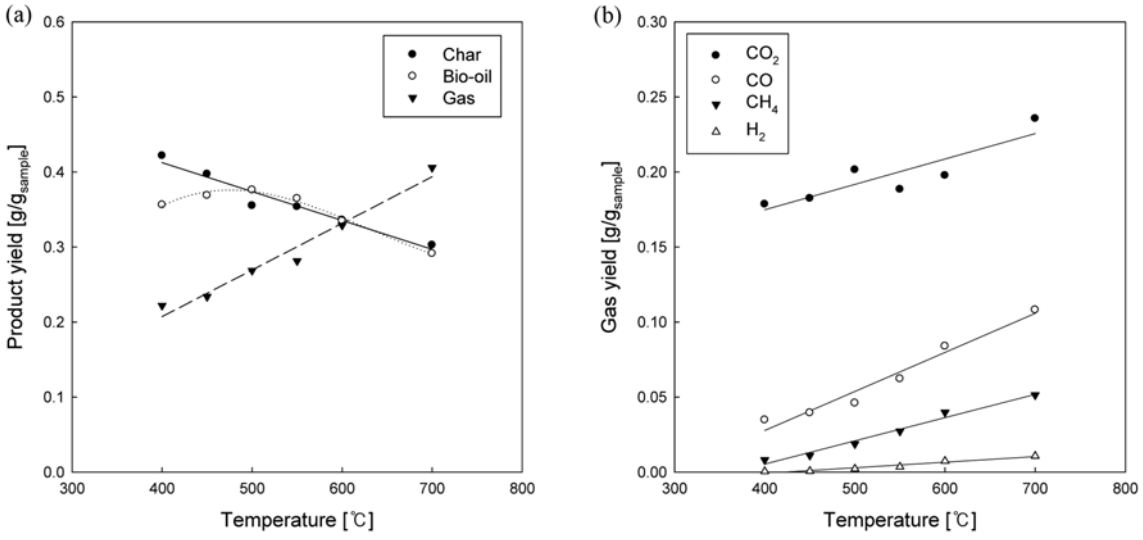

Fig. 6. Effect of temperature on the products distribution (a) and yield of gas components (b).

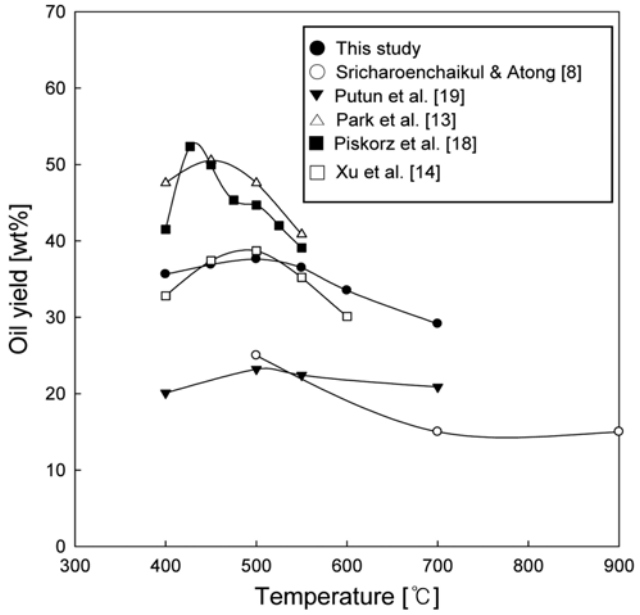

Fig. 7. Comparison of oil yields between present and previous studies.

ing temperature, heating rate, particle size, feed rate, reactor type, residence time of pyrolysis vapor and biomass species. As can be seen, oil yields are maximized at temperatures of 400-500 °C irrespective of various parameters. Oil yields from fluidized bed reactors are higher than those from fixed bed reactors. Fluidized bed reactors can offer more favorable conditions to produce bio-oil with high heat and mass transfer, uniform temperature and well sweeping condition [13,15,16]. Comparing the yields from fluidized bed reactors, oil yields in this study are relatively lower than others. As reported previously, oil yield from pyrolysis of agricultural waste like Jatropha residue is about 35-50 wt% lower than that from woody biomass (generally up to 80 wt%) due to high ash content [5,15, 16,20]. Since inorganic matters of ash enhance the formation of char and catalyze the conversion of vapors into gas, higher ash content induces higher char and gas yields but lower oil yields.

Ultimate analysis of bio-oil and char at different temperature is shown in Fig. 8(a). Carbon content in bio-oil has a maximum value of 49.2 wt% at 500 °C. With increasing temperature, conversion to gas increases, carbon content in bio-oil decreases over 500 °C; however, oxygen content has a minimum value of 36.8 wt%. The effect of temperature on the content of hydrogen and nitrogen is negligibly small about 9.3 and 4.7 wt%, respectively. On the other hand, carbon content in char increases but the amount of H_2 and O_2 decreases with increasing temperature over 500 °C. It may indicate that the amount of fixed carbon in char increases due to a secondary decomposition to produce residual volatiles at higher temperature. Sulfur in bio-oil and char was found to be less than 0.4 wt%

Table 3. Pyrolysis conditions of previous studies in Fig. 7

Authors	Feedstock	Reactor type (I.D.×high [m])	d_p [mm]	Gas flow rate	F_s [g/min] (input [g])
Sricharoenchaikul and Atong [8]	Jatropha seed shell	Fixed bed (ND[a])	-	0.0675 L/min	(ND)
Putun et al. [19]	Hazelnut shell	Flixed bed (0.11×0.80)	-	0.10 L/min	(3)
Park et al. [13]	Oriental white oak sawdust	Fluidized bed (0.08×0.3)	0.7	3 L/min	2.5 (150)
Piskorz et al. [18]	Sweet sorghum	Fluidized bed (ND[a])	ND[a]	ND[a]	0.17-1.67
Xu et al. [14]	Grape residue	Fluidized bed (0.078×0.52)	0.18	ND[a]	ND[a] (400)

[a]No data

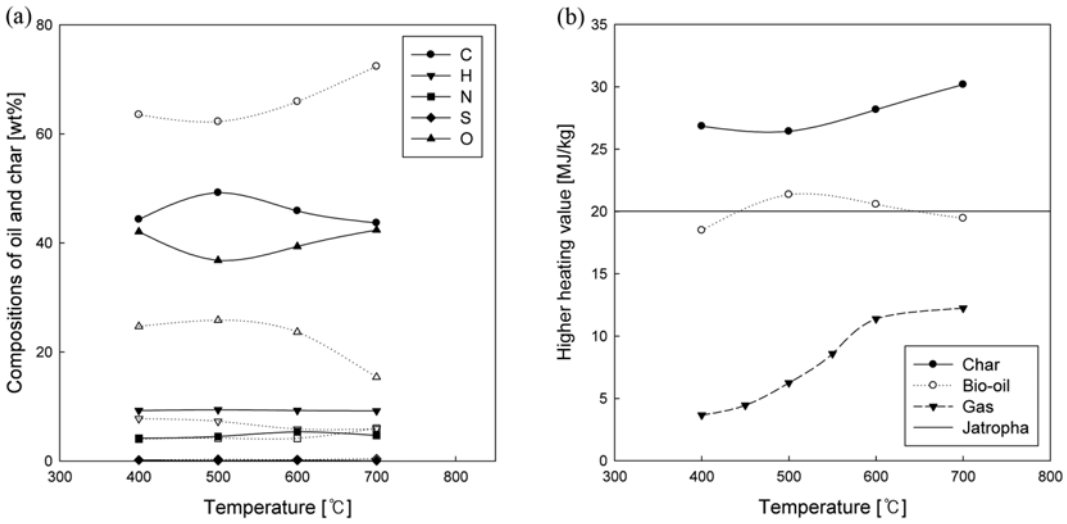

Fig. 8. Ultimate analyses of bio-oil (closed) and char (open) at different reaction temperature (a) and effects of temperature on higher heating values (b).

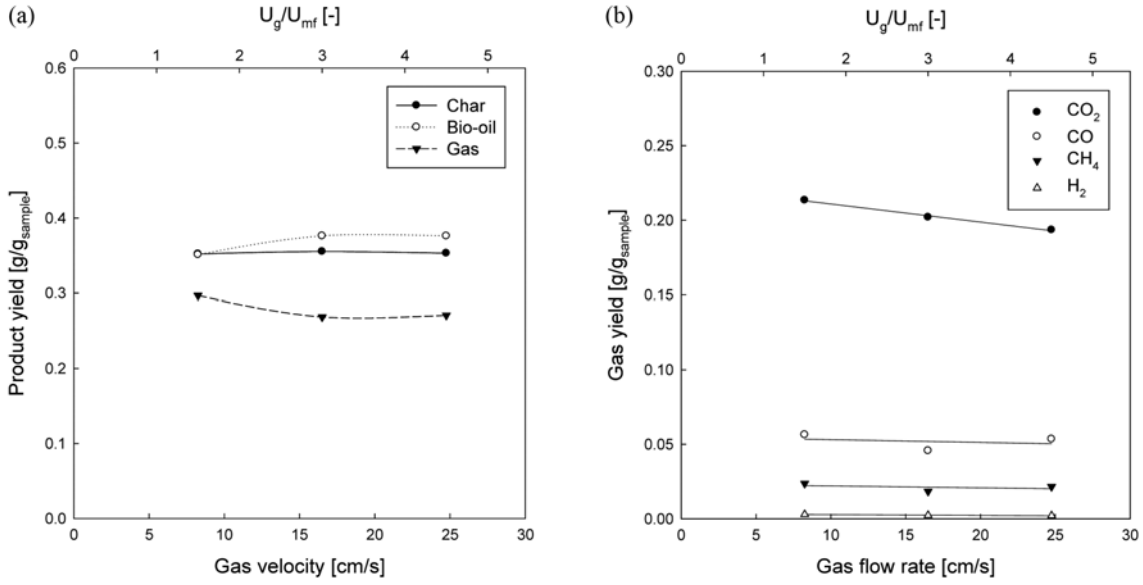

Fig. 9. Effect of gas velocity on the products distribution (a) and yield of gas components (b).

since Jatropha has low sulfur content. Higher heating values (HHVs) of each product at different temperature are shown in Fig. 8(b), where HHV of char was determined by Dulong equation [21]. HHVs of gas and char increased up to 12.2 and 30.2 MJ/kg at 700 °C due to increases in yield of combustible gases and fixed carbon at high temperature. However, HHV of bio-oil has a maximum value of 21.3 MJ/kg at 500 °C where carbon content reaches the maximum. In energy distributions of products based on HHV, char constitutes about 60% of overall energy at low temperature, while it decreases down to 45% with increase of temperature due to a decrease in char yield. However, energy proportion of gas products increases up to 25% with increase of temperature due to increases of gas yield and HHV. At 500 °C, bio-oil constitutes up to 40% of overall energy with a maximum of yield and carbon content.

2-2. Effects of Gas Flow Rate and Feedstock Particle Size

The effect of gas velocity on the product distribution and gas component yield from pyrolysis of Jatropha seedshell waste of a mean particle size of 6.0 mm at 500 °C is shown in Fig. 9. At lower gas velocity with longer residence time of volatiles, oil yield decreases due to an increase in secondary decompositions of oil products [12]. However, at higher gas velocity, vigorous bubbling action induces good contact between bed material and Jatropha waste [3,13]. This causes an increase in oil yield and a stable fluidization with higher mixing efficiency at gas velocity over $3U_{mf}$. With increasing gas velocity, the total gas yields and all the gas components decrease due to the decrease of secondary reactions of oil products as in Fig. 9. However, their effect on the weight fractions of gas components is small in the experimental range of this study.

The effect of feedstock particle size on the products distribution and gas component yields at 500 °C are shown in Fig. 10. An optimum condition to maximize the pyrolytic bio-oil yield is obtained at particle size of 1.7 mm. With increasing particle size larger than

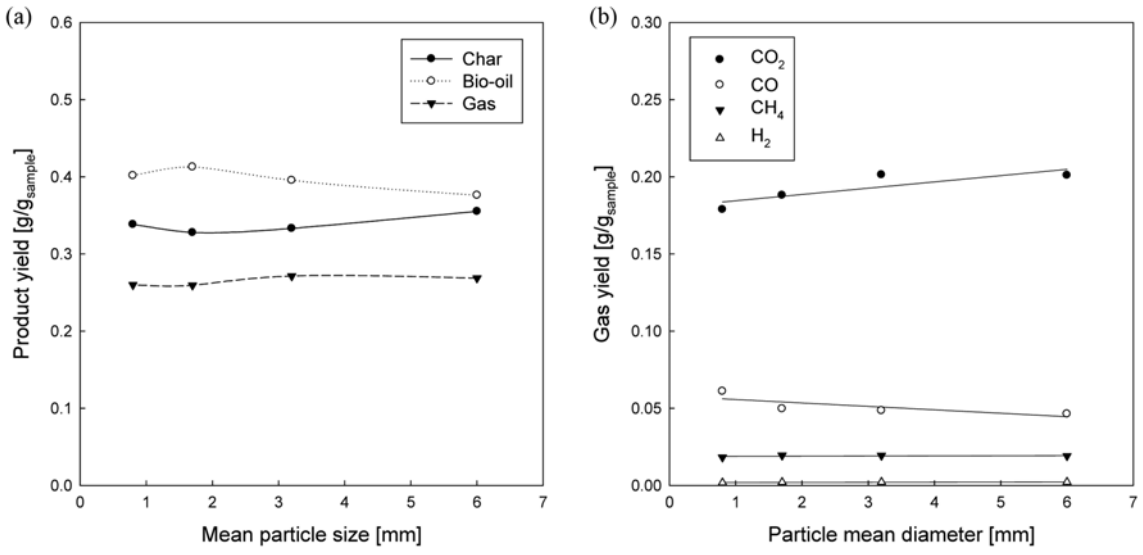

Fig. 10. Effect of feedstock particle size on the products distribution (a) and yield of gas components (b).

Table 4. Properties of pyrolytic bio oil and petroleum fuel oils (dry basis, wt%)

Properties	Pyrolytic oil (500 °C)	HS diesel	Heavy fuel oil (0.3S B-C)	Heavy fuel oil (4.0S B-C)
Elemental composition [wt%]				
C	49.19	85.90	87.30	82.79
H	9.40	12.98	12.19	12.98
O	36.81	0.10	0.17	0.48
N	4.51	0.57	0.06	0.20
S	0.09	0.46	0.28	3.55
H/C molar ratio	2.29	1.813	1.675	1.881
O/C molar ratio	0.56	<0.005	<0.005	<0.005
TAN [mg KOH/g]	64	0.25	0.451	N/A*
Specific gravity	1.03	0.87	0.94	0.98
HHV [MJ/kg]	21.3	39.1	44.7	43.4

*N/A=Not available

1.7 mm, bio-oil yield decreases while gas and char yields increase (Fig. 10(a)). Increase of feedstock size causes uneven temperature throughout the particle by low heating rate and longer residence time of volatile by the thick char layers to pass, resulting in a decrease in oil yield [12,13]. Smaller particles have higher reactivity than larger ones than 2.0 mm as shown in kinetic results in thermobalance reactor, but overheating the small particles causes a decrease in oil yield [3.13]. CO_2 yield increases up to 12% with increasing particle size (Fig. 10(b)), since larger particles may lead to a slow heating rate [12,13]. The effect of particle size on the yields of CH_4 and H_2 is negligibly small as 0.019 and 0.002 g/g_{sample}, respectively.

2-3. Comparison between Pyrolytic Oil and Petroleum Oils

One of target products in pyrolysis is pyrolytic bio oil because it has high applicability as an alternative to petroleum fuels. The properties of the pyrolytic oils and petroleum fuel oils are shown in Table 4. High-sulfur diesel and heavy fuel oils (Bunker-C oils) as petroleum fuel oils were chosen for comparison. The pyrolytic oil has higher oxygen content than the petroleum oils and shows lower higher heating value (HHV) and higher TAN (or lower pH) consequently. It indicates that the pyrolytic oil should be deoxygenated to get high HHV and low TAN for fuel application [22]. The pyrolytic oil shows lower sulfur and higher nitrogen content than petroleum oils. Its low sulfur content is positive for fuel application, though its high nitrogen content is not favorable due to causing NOx emission in fuel use. This implies that the pyrolytic oil should be denitrogenated before deoxygenation to improve its applicability as fuels [2]. The pyrolytic oil with wide distributions of compounds shows higher specific gravities than those of the petroleum oils.

Fig. 11 shows boiling point distributions of pyrolytic bio-oil and its comparison with petroleum fuel oils to provide information that the obtained oil corresponds to which petroleum fuel application. Pyrolytic oil showed wide distributions from 100 to 600 °C and a plateau region at *ca.* 360 °C, implying that several compounds were highly concentrated in the pyrolytic oil. As shown in chemical composition analysis of Table 2, Jatropha seed shell waste has a large portion of organic compounds like oil or fatty molecule because it is remnant from oil extraction. From GC/MS analysis, the main organic compounds in the pyrolytic oil are composed of 13.7 wt% of phenolic derivatives, 77.4 wt% of fatty acids and 6.8% of di- and triglycerides. The fatty acids have boiling points within 300-400 °C.

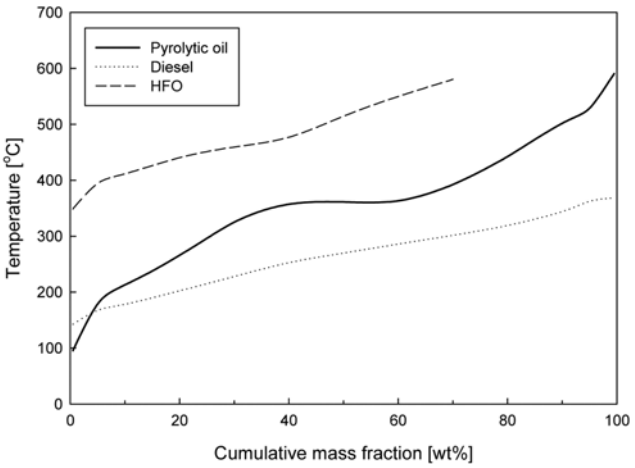

Fig. 11. Boiling point distributions of pyrolytic bio-oil and petroleum fuel oils.

In comparison with petroleum fuel oil, the distribution of pyrolytic oil covers the range of diesel and heavy fuel oil. Major portion of the pyrolytic oil is expected to be shifted possibly into the diesel range (less than 300 °C) if they are deoxygenated.

CONCLUSIONS

Pyrolysis kinetics of Jatropha seed shell waste is determined in a thermobalance reactor. It is found that the Avrami-Erofeev reaction model represents pyrolysis conversion of Jatropha well with the activation energy of 36.4 kJ mol^{-1} and frequency factor of 9.18 s^{-1}. The effects of reaction temperature, gas flow rate and feedstock particle size on products distribution have been determined. With increasing pyrolysis temperature, char yield decreases while carbon content in char increases. The total gas yield and combustible gas fraction increase rapidly with increasing temperature. Char and gas yields increase and oil yield decreases with decrease of gas velocity under $3U_{mf}$ and increase of feedstock particle size over 1.7 mm. A condition to maximize the pyrolytic bio-oil yield is obtained at 500 °C with gas velocity higher than $3U_{mf}$ and feedstock particle size of 1.7 mm, where the carbon content in bio-oil and higher heating value

shows their maximum values. The pyrolytic oil is characterized by more oxygen, lower HHVs, less sulfur and more nitrogen than petroleum fuel oils. The pyrolytic oil showed plateaus around 360 °C in distribution of components' boiling point due to high yields of fatty acid and glycerides.

ACKNOWLEDGEMENTS

The authors acknowledge a grant-in-aid for research from SK innovation.

REFERENCES

1. Y. Kim, H. W. Lee, S. Lee, S. Kim, S. H. Park, J. Jeon, S. Kim and Y. Park, *Korean J. Chem. Eng*., **28**, 2012 (2011).
2. S. W. Kim, B. S. Koo, J. W. Ryu, J. S. Lee, C. J. Kim, D. H. Lee, G. R. Kim and S. Choi, *Fuel Process. Technol*., **108**, 118 (2013).
3. M. N. Islam, R. Zailani and F. N. Ani, *Renew. Energy*, **17**, 73 (1999).
4. H. S. Choi, Y. S. Choi and H. C. Park, *Korean J. Chem. Eng*., **27**, 1164 (2010).
5. J. Yanik, C. Kornmayer, M. Saglam and M. Yuksel, *Fuel Process. Technol*., **88**, 942 (2007).
6. A. Caglar and A. Demirbas, *Energy Convers. Manage*., **43**, 489 (2002).
7. J. M. Encinar, J. F. Gonzalez, G. Martinez and J. M. Gonzalez, *Fuel Process. Technol*., **89**, 1448 (2008).
8. V. Sricharoenchaikul and D. Atong, *J. Anal. Appl. Pyrol*., **85**, 155 (2009).
9. S. Vyazovkin and C. A. Wight, *Thermochim. Acta*, **340-1**, 53 (1999).
10. Y. C. Kim, S. Kim and S. H. Chung, *J. Ind. Eng. Chem*., **11**, 857 (2005).
11. T. W. Kwon, S. D. Kim and D. P. C. Fung, *Fuel*, **67**, 530 (1988).
12. H. Zhang, R. Xiao, H. Huang and G. Xiao, *Bioresour. Technol*., **100**, 1428 (2009).
13. H. J. Park, Y. Park, J. Dong, J. Kim, J. Jeon, S. Kim, J. Kim, B. Song, J. Park and K. Lee, *Fuel Process. Technol*., **90**, 186 (2009).
14. R. Xu, L. Ferrante, C. Briens and F. Berruti, *J. Anal. Appl. Pyrol*., **86**, 58 (2009).
15. C. D. Blasi, G. Signorelli, C. D. Russo and G. Rea, *Ind. Eng. Chem. Res*., **38**, 2216 (1999).
16. Z. Luo, S. Wang, Y. Liao, J. Zhou, Y. Gu and K. Cen, *Biomass Bioenerg*., **26**, 455 (2004).
17. T. Sonobe, N. Worasuwannarak and S. Pipatmanomai, *Fuel Process. Technol*., **89**, 1371 (2008).
18. J. Piskorz, P. Majerski, D. Radlein, D. S. Scott and A. V. Bridgwater, *J. Anal. Appl. Pyrol*., **46**, 15 (1998).
19. A. E. Putun, A. Ozcan and E. Putun, *J. Anal. Appl. Pyrol*., **52**, 33 (1999).
20. L. Conti, G. Scano and J. Boufala, *Biomass Bioernerg*., **7**, 291 (1994).
21. D. M. Mason and K. N. Gandhi, *Fuel Process. Technol*., **7**, 11 (1983).
22. H. J. Park, J. K. Jeon K. Y. Jung, Y. S. Ko, J. M. Sohn and Y. K. Park, *Korean Chem. Eng. Res*., **45**, 340 (2007).